SC-4691(RR)

COMPILATION AND CORRELATION OF MODEL STARTING LOADS FROM SEVERAL SUPERSONIC WIND TUNNELS

R. C. Maydew - 7132

June 1962

ABSTRACT

Normal- and axial-force starting and stopping loads were measured on eight axisymmetric models in a perforated-wall test section, blowdown wind tunnel at nominal Mach numbers of 2, 2.5, and 3. These transient normal-force data correlate fairly well with data from five other supersonic tunnels, for a variety of model shapes, when the total model planform area and the stagnation pressure at tunnel start are used to nondimensionalize the loads. An empirical method for predicting normal-force starting loads is developed.

Issued by Sandia Corporation,
a prime contractor to the
United States Atomic Energy Commission

LEGAL NOTICE

This report was prepared as an account of Government sponsored work. Neither the United States, nor the Commission, nor any person acting on behalf of the Commission:

A. Makes any warranty or representation, expressed or implied, with respect to the accuracy, completeness, or usefulness of the information contained in this report, or that the use of any information, apparatus, method, or process disclosed in this report may not infringe privately owned rights; or

B. Assumes any liabilities with respect to the use of, or for damages resulting from the use of any information, apparatus, method, or process disclosed in this report.

As used in the above, "person acting on behalf of the Commission" includes any employee or contractor of the Commission, or employee of such contractor, to the extent that such employee or contractor of the Commission, or employee of such contractor prepares, disseminates, or provides access to, any information pursuant to his employment or contract with the Commission, or his employment with such contractor.

Printed in USA. Price $0.75. Available from the Office of Technical Services, Department of Commerce, Washington 25, D. C.

TABLE OF CONTENTS

	Page
Nomenclature	5
Summary	7
Introduction	9
Other Studies	10
General	10
"Normal-Shock" Method	10
Test Equipment	11
Wind Tunnel	11
Models	14
Balance and Sting Configurations	15
Instrumentation	16
Procedure	18
Test Procedure	18
Data Reduction	18
Discussion of Results	19
Axial Loads	19
Normal Loads	21
Normal Shock Method Modification	24
Frequency and Damping Effects	27
Conclusions	29
List of References	30

LIST OF ILLUSTRATIONS

Figure		Page
1	Sandia 1-Foot Trisonic Wind Tunnel	11
2	Tunnel Test and Nozzle Sections with Plenum Door Retracted	12
3	Typical Centerline Mach Number Distributions	13
4	Model Configurations	14
5	SC-3C-3 Balance-Sting Installation in Tunnel	15
6	SC-3C-5 Balance and Support Sting	16
7	Typical Oscillograph Records of Normal and Axial Forces, Configuration 8, M = 2	17
8	Range of Maximum Measured Axial-Force Starting and Stopping Loads	19
9	Effect of Mach Number and Model Shape on the Ratio of Starting to Steady-State Axial-Force Loads	20
10	Range of Maximum Measured Normal-Force Starting and Stopping Loads	21
11	Effect of Mach Number and Model Shape on Ratio of Starting to Steady-State Normal-Force Loads	22
12	Effect of Mach Number and Model Shape on Ratio of Stopping to Steady-State Normal-Force Loads	23
13	Range of Measured Normal-Force Starting Loads (comparison with AEDC data and empirical method)	25
14	Comparison of Experimental Data with Modified Normal-Shock Methods	25
15	Correlation of Experimental Data with Modified Normal-Shock Method	26
16	Comparison of the Measured Frequency Ratios and Damping Factors with Ratios for a Forced-Vibration (with viscous damping) System	28

LIST OF TABLES

Table		Page
I	Model Dimensions	14
II	Wind-off Natural Frequency and Damping of Sting-Balance-Model Configurations	16
III	Schedule of Runs	18
IV	Forcing Frequency Data	27

NOMENCLATURE

A - model axial force during steady supersonic flow, lbs

A_1 - test section cross-sectional area, in.^{2}

A_d - balance axial-force design loading, lbs

A_f - total ejector open area (see Figure 5), in.^{2}

A_m - maximum model axial force during tunnel start, lbs

A_s - model axial force during tunnel start or stop, lbs

b - damping factor (Equation 5), dimensionless

C_{Am} - maximum axial-force coefficient during tunnel start, A_m/q_sS

C_A - axial-force coefficient during steady supersonic flow, A/qS

C_{Nm} - maximum measured normal-force coefficient during tunnel start or stop, $N_m/P_{ts}S_t$

C_{Nc} - computed maximum normal-force coefficient during tunnel start (Equations 1 and 4)

C_{N10} - normal-force coefficient at $\alpha = 10$ degrees during steady supersonic flow, N_{10}/P_tS_t

C_s - computed maximum normal-force coefficient during tunnel start (normal-shock method, Equation 2)

d - reference or forebody model diameter, inches

d_m - maximum model diameter, inches

f_a - model-balance natural frequency in axial direction, cps

f_f - forcing frequency (test section pressure oscillation), cps

f_{n1} - model-balance natural frequency normal to model in pitch plane, cps

f_{n2} - sting natural frequency normal to model in pitch plane, cps

FR - model fineness ratio in calibers, ℓ/d

ℓ - model length, inches

m_d - balance pitching moment (about balance center) design loading, in.-lbs

M - Mach number

N - model measured normal force during start or stop, lbs

N_s - computed maximum normal force during tunnel start (normal-shock method, Equation 2), lbs

N_c - computed maximum normal force during tunnel start (Equations 1 and 4), lbs

N_d - balance normal-force design loading, lbs

NOMENCLATURE (continued)

N_m - maximum normal force during tunnel start or stop, lbs

N_{10} - normal force with model at α = 10 degrees during steady supersonic flow, lbs

P_t - stagnation pressure, psia

P_{ts} - stagnation pressure at tunnel start, psia

q - dynamic pressure during steady-state operation, psi

q_s - dynamic pressure at tunnel start, psi

R.M. - relative load magnification factor

S - model cross-sectional area (based on d), in.^{2}

S_m - maximum model cross-sectional area (based on d_m), in.^{2}

S_L - model exposed lifting surface area (projected with fins in + position, in.^{2})

S_T - total model planform area, in.^{2}

β - exponent defined by Equation 4a

θ - amplitude of oscillation, degrees

γ - ratio of specific heats

SUMMARY

Comparison of normal-force starting load data measured on 13 model shapes in 6 supersonic wind tunnels indicate fair correlation when the model planform area (rather than lifting surface area) and the stagnation pressure at tunnel start are used to nondimensionalize the loads. The data indicate that the normal-force starting loads are a function of the ratio of model lifting surface area to total planform area. An empirical modification of the "normal-shock" method is developed; this method approximates the maximum normal-force starting loads measured at several supersonic wind tunnels.

A limited amount of axial- and normal-force starting and stopping load data were obtained in the Sandia 1- by 1-foot intermittent, trisonic wind tunnel. Eight axisymmetric models were tested at zero angle of attack at nominal Mach numbers of 2, 2.5, and 3. The maximum axial- and normal-force starting loads were higher than the stopping loads. The maximum axial-force starting load at $M = 3$ was approximately 3-1/2 times the steady running load at $\alpha = 0$ degrees. The maximum normal-force starting load at $M = 3$ and $\alpha = 0$ degrees was approximately 5 times the steady running load at $\alpha = 10$ degrees. The models oscillated at the system natural frequencies during the starting and stopping transients. Measurements of test section pressure transients during tunnel start indicated symmetrical starts at $M = 2$ and fore and aft oscillation of the shock system at $M = 2.5$ and $M = 3$.

ACKNOWLEDGMENT

Appreciation is expressed to M. W. Williams (formerly with Sandia Laboratory) and E. A. Koenig for conducting these tests.

COMPILATION AND CORRELATION OF MODEL STARTING LOADS FROM SEVERAL SUPERSONIC WIND TUNNELS

Introduction

During the starting of a supersonic tunnel, the air flow must be accelerated from subsonic to supersonic in the test section. The ideal model of the starting process for inviscid flow consists of formation of a normal shock at the nozzle throat (as the tunnel stagnation pressure is increased) and the steady travel of the normal shock down the nozzle across the model and into the diffuser. The actual starting process is characterized by random, viscous-induced flow separation in the nozzle, resulting in the unsteady passage of oblique and/or normal shock waves over the model. The unsteady longitudinal and lateral oscillation of the waves result in large local flow inclinations at the model. These flow inclinations, coupled with the pressure change across the waves, result in excessive model loads during the starting process. A somewhat similar phenomenon occurs during the stopping process, as the test section flow breaks down from supersonic to subsonic.

Wind-tunnel operators have been aware of this starting load phenomenon for many years. Some of the earlier supersonic tunnels were intermittent, vacuum-indraft facilities. Since the magnitude of the starting loads is proportional to the starting density, excessive model loads were not encountered in the indraft facilities. During the last several years (with the placing in operation of several large, atmospheric-exhaust, blowdown supersonic tunnels[1,2]) the starting load problem has been investigated more thoroughly because of the damage to internal strain gage balances, models, etc. Unfortunately, however, the results of most of these studies are not available in the open literature.

Gorowitz[1] indicated that a hangar (mounted in the model support sector, into which the model is retracted and clamped during periods of transient flow) has been developed for model protection at the 7-foot trisonic tunnel at North American. Schreiber[2] reported that proximity plates (which are retracted into the top and bottom test section walls during steady flow conditions) support the model during the starting and stopping of the Boeing 4-foot supersonic tunnel. These extensive model-protection measures indicate the severity of the transient loading problem for atmospheric-exhaust supersonic wind tunnels.

The testing capability of the Sandia 1-foot trisonic blowdown tunnel was extended to $M = 3$ in April 1960. Force tests of axisymmetric models (bodies of revolution with flared afterbodies or low-aspect ratio fins) resulted in model or balance damage. Available analytical methods ("normal-shock"[3] and Winter and Brown[4]) were not suitable for predicting transient loads on these axisymmetric shapes, since these methods were developed for winged (lifting) vehicles. Hence, a limited experimental investigation to measure the transient normal and axial forces on eight typical models was undertaken. Four configurations were tested at Mach number 2, two at Mach number 2.5, and seven at Mach number 3.

The purpose of this report is to correlate the available starting load data from other supersonic tunnels with the present results and to develop an empirical method for predicting normal-force starting loads for a variety of model shapes.

Other Studies

General

An excellent description of the nozzle-starting characteristics, tunnel wave mechanics, and transient sequence for atmospheric-discharge blowdown tunnels is given by Schreiber[2]. Schreiber indicated that a large number of starting load tests had been conducted in the Boeing 4-foot and 1/10-scale supersonic tunnels at Mach numbers up to 4; however, these data have not been found in the open literature.

Goin[5] presents some starting load data taken on a body alone, a wing alone, and a wing-body combination at $\alpha = 0$ degrees at Mach numbers of 1.5 to 2.75 in the Ordnance Aerophysics Laboratory continuous tunnel. These data were presented as the ratio of starting or stopping loads to steady-state loads at $\alpha = 10$ degrees and $\alpha = 0$ degrees for normal forces and axial forces, respectively.

Kinsolving and Jackson[3] investigated the effect of starting density, model orientation (pitch, roll, yaw), and support-system frequency on the peak starting loads of an AGARD Model B in a 12-inch wind tunnel at Mach numbers of 2.0, 3.0, and 4.5. These authors concluded that there was no consistent variation of measured peak loads with either support-system frequency or model attitude; however, the peak loads increased directly as the starting density and the "normal-shock" prediction (Equation 1) approximated the maximum normal-force loads except at Mach number 2.

Gorowitz[1] investigated the effect of the ratio of exposed projected lifting surface area to total model projected area on the normal-force starting load at Mach numbers of 2.0, 2.5, and 3.0 in the North American 7-foot trisonic tunnel. Models of area ratios of 0 (body of revolution), 0.18, 0.42, 0.55, and 1.0 (wing alone) were tested. The North American data showed a linear increase in normal-force starting loads with area ratio.

The results of several starting load studies have been reported at informal Supersonic Tunnel Association meetings; however, these data are not available in the open literature.

"Normal-Shock" Methods*

This method assumes that during the transient starting process it is possible (for brief periods) to have supersonic flow established over the top surface of a wing and a normal shock standing at the leading edge on the bottom surface. Subsonic flow is assumed to exist behind the shock on the lower wing surface. This condition would result in a low pressure on the upper surface and a high pressure on the lower surface. If the wing is assumed to be an infinite aspect ratio, thin flat plate at zero angle of attack (with the pressures constant over the wing surfaces), then the normal force can be expressed as:

$$N_s = P_{ts} S_L \frac{2\gamma(M^2 - 1)}{(\gamma + 1)\left(1 + \frac{\gamma - 1}{2} M^2\right)^{\frac{\gamma}{\gamma - 1}}} \tag{1}$$

or

$$C_s = \frac{N_s}{P_{ts} S_L} = \frac{2\gamma(M^2 - 1)}{(\gamma + 1)\left(1 + \frac{\gamma - 1}{2} M^2\right)^{\frac{\gamma}{\gamma - 1}}} \tag{2}$$

*This method, to the best of the author's knowledge, was first proposed by D. H. Ross, Naval Supersonic Laboratory, MIT, in 1956.

This approximate method has been used by several wind-tunnel operators as a guide for comparison of starting load data and/or for calculating loads for design purposes. However, the above equations cannot be used for estimating the starting loads on a flare-stabilized body of revolution, since the lifting surface area (S_L) is zero. Hence, for more general application of this method, it is proposed that the total model planform area (S_T), rather than the lifting surface area (S_L), be used to define the normal-force coefficient. This approach would allow a more meaningful comparison of the starting load data from a variety of model shapes; therefore, the normal-shock method referred to hereafter in this report is defined as:

$$C_{Nc} = \frac{N_c}{P_{ts} S_T} = \frac{2\gamma(M^2 - 1)}{(\gamma + 1)\left(1 + \frac{\gamma - 1}{2} M^2\right)^{\frac{\gamma}{\gamma - 1}}} . \tag{3}$$

Test Equipment

Wind Tunnel

A sketch, showing the general arrangement of the Sandia trisonic wind tunnel, is presented in Figure 1. The tunnel is an intermittent, atmospheric-exhaust, blowdown type with a 1- by 1-foot perforated-wall test section. Dry air at 300 psi is stored in two 2600-foot^3 tanks; heat storage material (tin cans) in the tanks minimize the temperature drop of the air during a 20- to 30-second run. The mass flows vary from approximately 30 to 100 pounds per second.

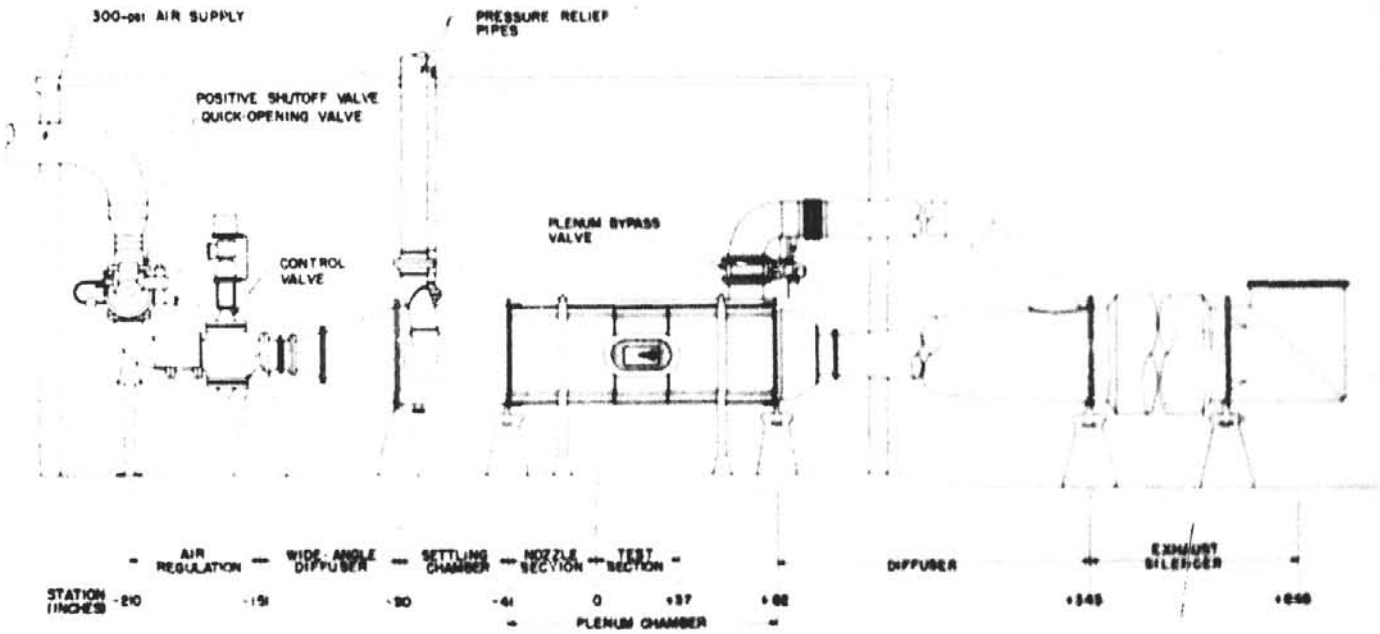

Figure 1. Sandia 1-Foot Trisonic Wind Tunnel

The air-regulating system consists of a positive shutoff wedge-gate valve, a quick-opening (0.4 second) butterfly valve and a control valve. The electrically operated gate valve provides personnel safety during model changes. The pneumatically operated butterfly valve is used to start (and stop) the tunnel with the control valve pre-positioned to the control point to minimize the starting transient. The stem motion of the double-port control valve is actuated by a pneumatic, piston-type operator. The Taylor pneumatic, pressure-control system maintains the settling chamber pressure to within approximately one-fourth to one-half percent of the set point during a run. The tunnel is operated at total pressures of 15 to 75 psia.

A series of screens in the wide-angle diffuser and settling chamber provide a uniform velocity distribution and relatively low turbulence level in the settling chamber.

Interchangeable nozzle block assemblies (sonic and nominal $M = 1.6$, 2.0, 2.5, and 3.0) are used with the perforated-wall test section (Figure 2). Test section Mach numbers from 0.5 to 1.35 can be generated with the sonic nozzle blocks. The porosity of the walls is 6 percent, with the holes inclined 60 degrees from the normal. The top and bottom perforated walls can be converged or diverged 60 minutes. Four manually adjustable ejector flaps (located at tunnel station 37) provide the pumping action to pull air through the perforated walls; this ejector flow re-enters in the diffuser section. The plenum bypass line is used to provide additional plenum pumping for obtaining Mach numbers of 1.1 to 1.35 with the sonic blocks.

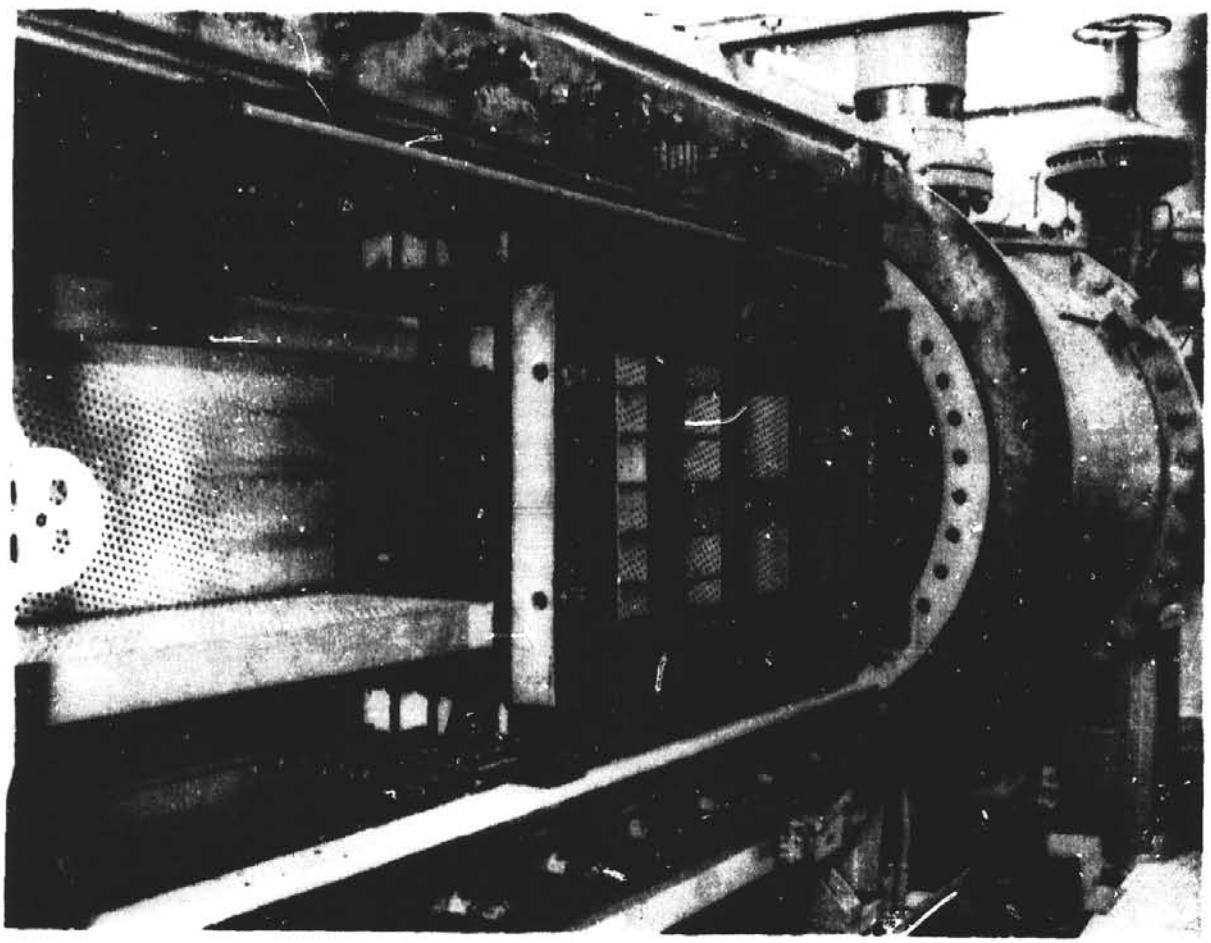

Figure 2. Tunnel Test and Nozzle Sections with Plenum Door Retracted

A vertical-strut mechanism allows pitching sting-mounted models from minus 7-degree to plus 13-degree angle of attack at a rate of 1.2 degrees per second. A choke assembly, consisting of a remotely translatable center body, is mounted in a cylindrical section downstream of the pitching strut. The primary function of the choke is to vary Mach number subsonically by choke-area changes; however, this assembly also provides supersonic diffusion when testing at the higher Mach numbers. A 8-degree conical subsonic diffuser is downstream of the choke assembly. A detailed description of the transonic tunnel, as originally built, is given by Davis and Peterson[6] and by Tolbert[7].

Typical test-section centerline Mach number distributions are presented in Figure 3.

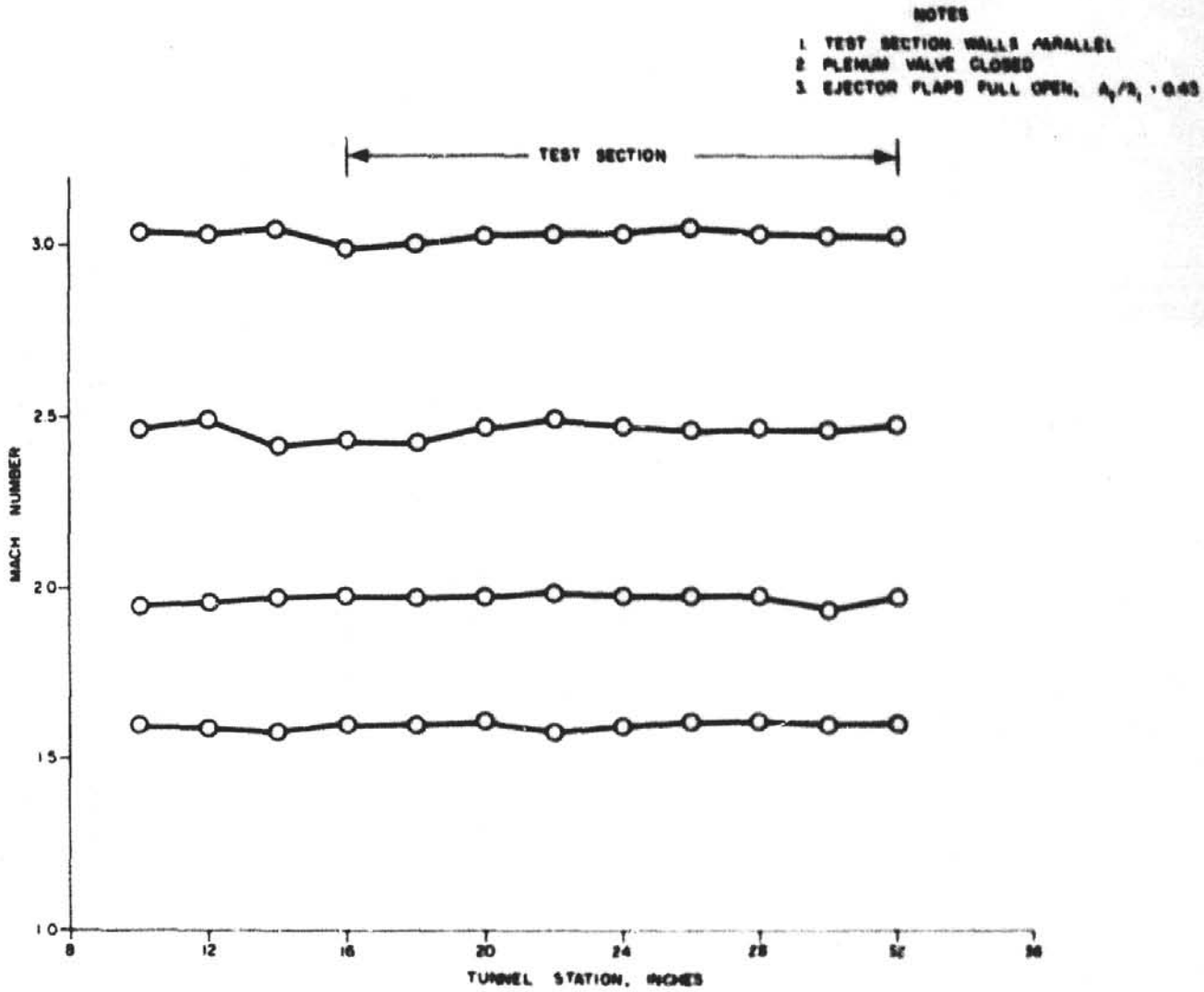

Figure 3. Typical Centerline Mach Number Distributions

Models

Seven of the eight models tested are presented in Figure 4, and pertinent model dimensions and areas are presented in Table I. Configurations 4, 6, and 7 were tested with the cruciform fins in the plus (+) position; i.e., one set in the vertical plane. The three-finned configurations, 3 and 8, were tested with one fin below centerline in the vertical plane.

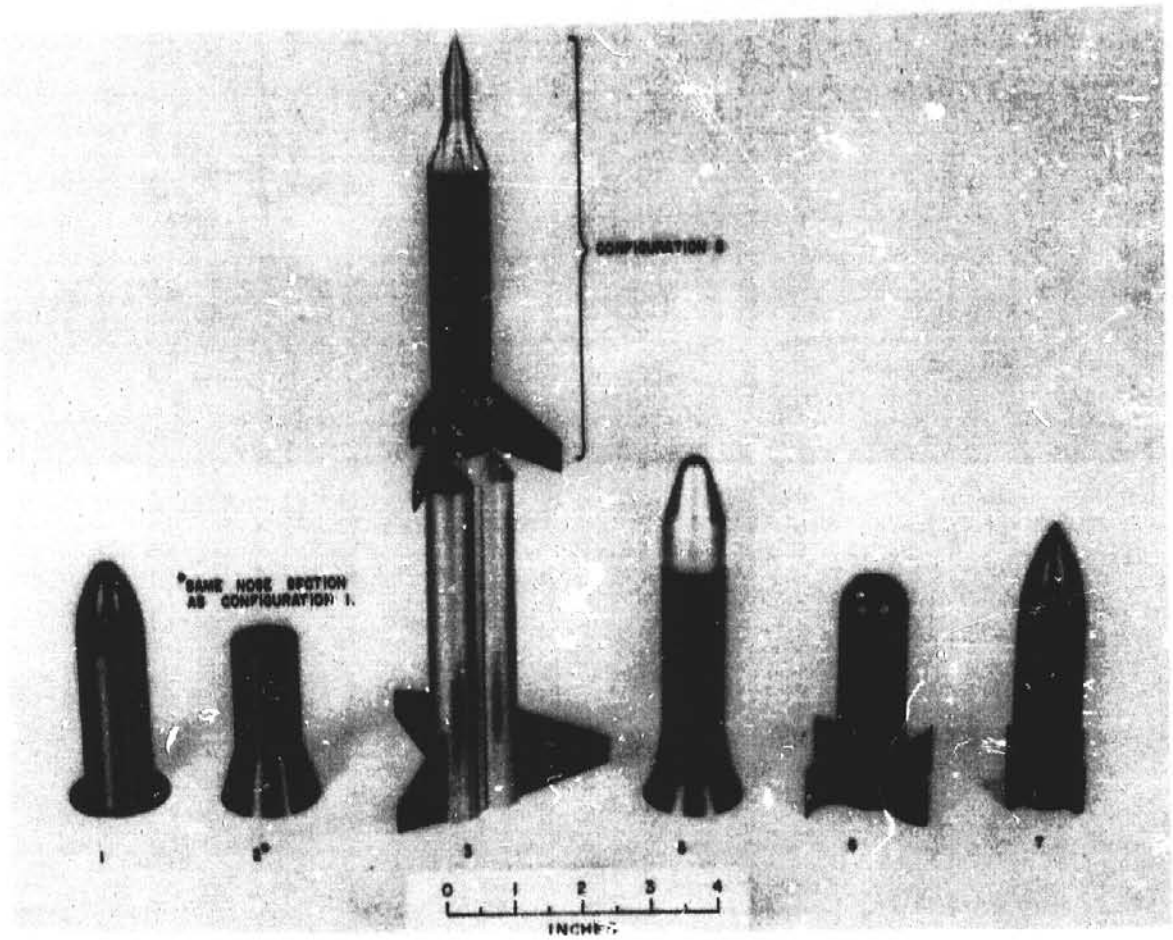

Figure 4. Model Configurations

TABLE I

Model Dimensions

Configuration	d, in.	d_m, in.	ℓ, in.	FR	S, in.^{2}	S_L, in.^{2}	S_T, in.^{2}	S_L/S_T
1	1.100	1.625	4.178	3.80	0.95	0	4.28	0
2	1.100	1.622	4.178	3.80	0.95	0	4.63	0
3	1.550	1.550	13.07	8.8	1.90	4.20	19.3	0.22
4	1.375	1.444	4.070	2.96	1.49	0.60	6.18	0.10
5	1.055	1.650	5.962	5.65	0.88	0	6.02	0
6	1.125	1.125	3.785	3.36	0.99	1.29	5.50	0.23
7	1.125	1.125	4.815	4.28	0.99	0.52	5.27	0.10
8	0.868	0.868	6.831	7.87	0.59	1.60	7.18	0.22

Balance and Sting Configurations

Two three-component strain gage balance-support sting configurations were used. A tunnel installation of the SC-3C-3 balance (used with configurations 1, 2, 4, 5, 6, and 7) is shown in Figure 5. Configurations 3 and 8 were tested with the SC-3C-5 balance shown in Figure 6.

The design specifications of the balances are:

Balance	Dia., in.	N_d, lbs	A_d, lbs	d, in.-lbs	Design Stress, psi
SC-3C-3	0.75	120	28	170	35,000
SC-3C-5	0.58	65	43	130	40,000

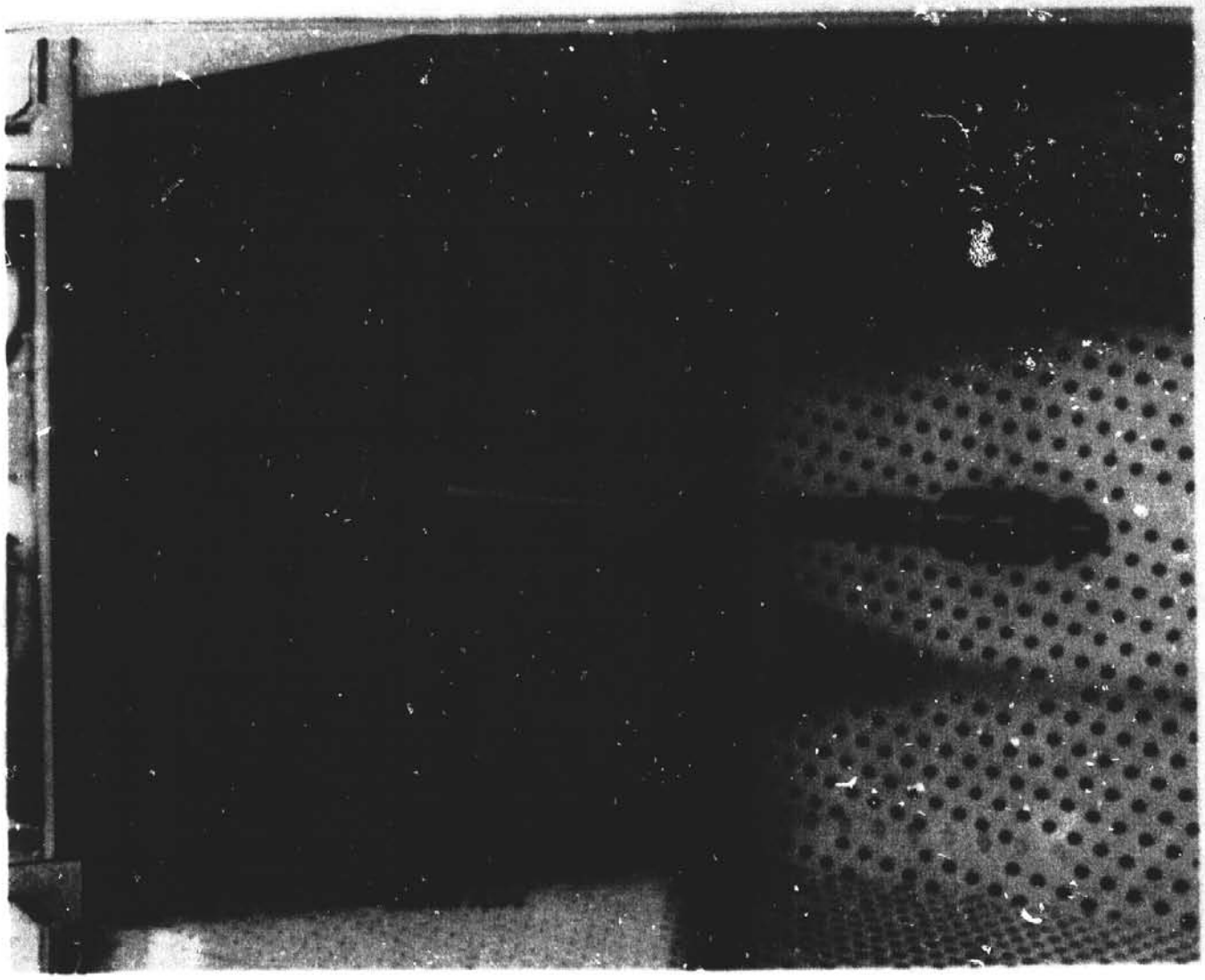

Figure 5. SC-3C-3 Balance-Sting Installation in Tunnel

Figure 6. SC-3C-5 Balance and Support Sting

Measurements of both axial and normal force were made, with the moment gages wired so that normal forces were measured directly. The natural frequencies of the model-balance configurations are listed in Table II.

TABLE II

Wind-off Natural Frequency and Damping of Sting-Balance-Model Configurations

Configuration	Balance	f_a, cycles/sec	f_{n1}, cycles/sec	f_{n2}, cycles/sec	b
1	SC-3C-3	1200	89	970	0.038
2	SC-3C-3	1190	90	880	0.044
3	SC-3C-5	540	37	700	0.047
4	SC-3C-3	470	47	710	0.014
5	SC-3C-3	790	76	940	0.020
6	SC-3C-3	620	58	970	0.019
7	SC-3C-3	570	56	940	0.015
8	SC-3C-5	890	66	800	--

Instrumentation

The balance strain gage outputs were recorded on a direct-writing Visicorder oscillograph (using 3.3-kc galvanometers) coupled to a 20-kc CEC carrier amplifier. This combination provided a flat frequency response up to approximately 1600 cycles per second. The Visicorder was operated at a paper speed of 25 inches per second. The settling chamber pressure (transient and steady-state) was measured with a 100-psia strain gage transducer; the output was recorded on a self-balancing 1-second (full-scale response time) strip chart recorder. The stagnation pressure transient signal lagged behind the oscillograph traces; however, this lag did not appreciably affect the accuracy of the measurements.

Typical normal- and axial-force oscillograph traces of starting and stopping are presented in Figure 7. The accuracy in the measurement of peak loads is approximately ±10 percent.

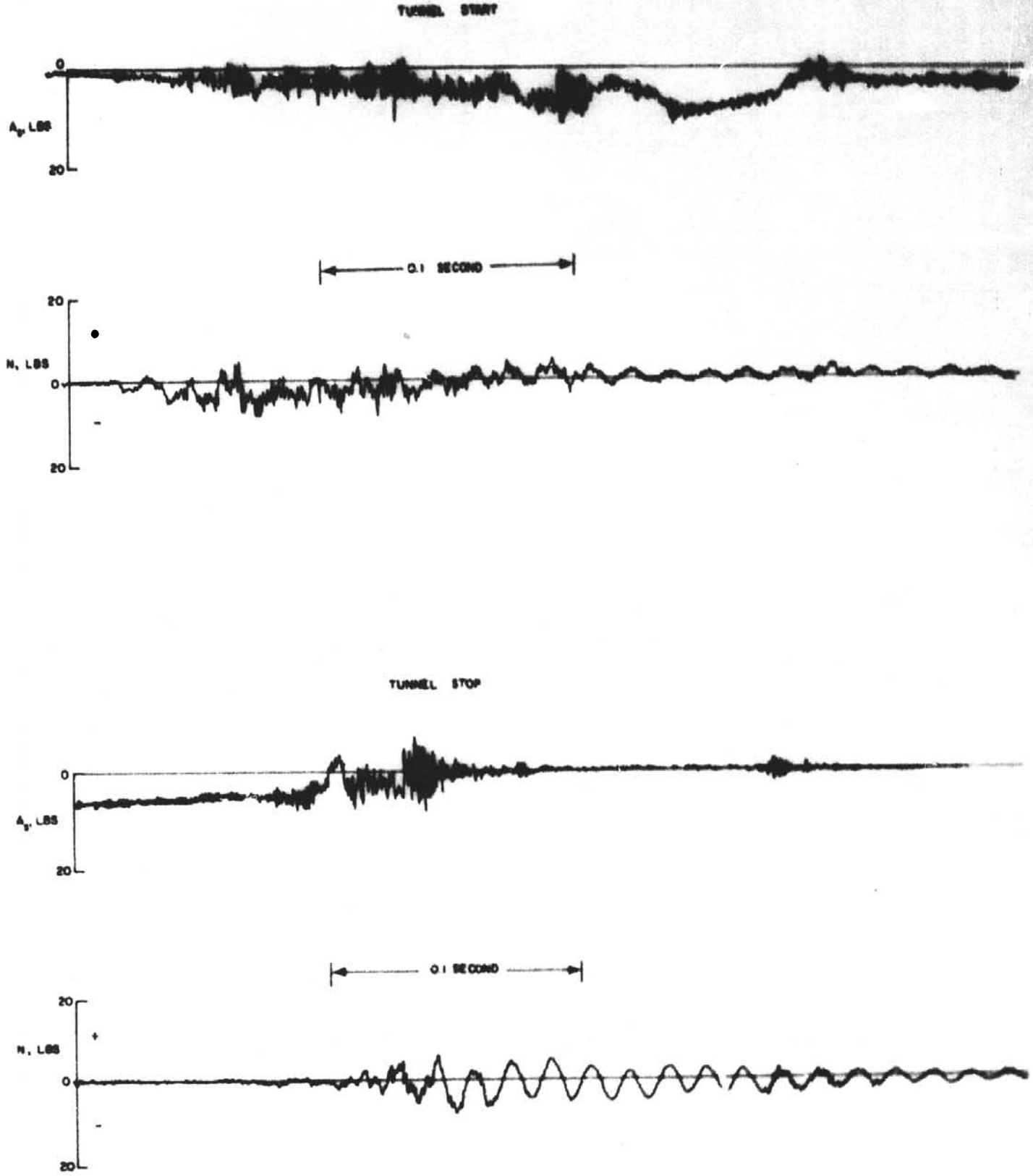

Figure 7. Typical Oscillograph Records of Normal and Axial Forces, Configuration 8, M = 2

Procedure

Test Procedure

A summary of the tests conducted is presented in Table III. Since the magnitude of starting loads—even with identical tunnel operating conditions—varies in a random fashion, a statistical approach is required. The lack of available wind-tunnel test time, plus the need to test several configurations, severely limited the number of runs that could be made under similar test conditions. Hence, it is possible that the maximum transient loads (especially normal-force) that might be encountered for these configurations have not been determined.

The test procedure consisted of (1) pre-positioning the control valve, (2) simultaneously starting the Visicorder and strip chart recorders and energizing the quick-opening valve, and (3) manually operating the pressure control system until the set point was reached, and then (4) switching over to the automatic operation of the pressure control system.

The starting times varied from approximately 0.4 to 0.7 second at M = 2, 0.5 to 1.0 second at M = 2.5, and 4.5 to 10 seconds at M = 3.0. The stopping times were approximately 0.25, 0.25, and 0.60 second at Mach numbers of 2, 2.5, and 3, respectively. The tunnel started at nominal stagnation pressures of 26, 41, and 55 psia at Mach numbers of 2, 2.5, and 3, respectively. The normal running stagnation pressures are 30, 45, and 70 psia at these Mach numbers. The long starting time at Mach 3 is a tunnel operating limitation. The tunnel must be started slowly at M = 3 to avoid a stagnation pressure overshoot which would rupture the 82-psia blowoff diaphragms (Figure 1).

TABLE III

Schedule of Runs

Configuration	M = 2	M = 2.5	M = 3
1	2	12	2
2	2	2	2
3	2	--	2
4	--	--	4
5	--	--	2
6	--	--	4
7	--	--	2
8	2	--	--

Data Reduction

Maximum values of normal force (both positive and negative) and axial force during starting and stopping were measured from the oscillograph records, using previously determined calibration constants. The steady-state axial loads were measured at three points on the oscillograph traces. The frequency of oscillation of the normal and axial forces were measured from the oscillograph records at the maximum transient load condition and during steady state. The starting and stopping times were estimated from the Visicorder traces.

The minimum stagnation pressure at which supersonic flow was established was determined for each tunnel start. These pressures were measured from the strip chart records, using the starting times determined from the oscillograph records. Arithmetic averages of these starting pressures (26, 41, and 55 psia at M = 2, 2.5, and 3, respectively) were used to calculate the normal-force coefficients.

Discussion of Results

Axial Loads

The range of maximum measured axial loads for the eight configurations at the three test Mach numbers is presented in Figure 8. Each block or bar represents the variation in the maximum transient loads for the number of runs shown in Table III. The starting loads were consistently higher than the stopping loads. The effect of model size and shape on the magnitude of the loads is relatively small. Note that the total spread of starting loads for configuration 1 at M = 2.5 (data from 12 runs) is no greater than the data spread for other test conditions where only 2 or 4 runs were made.

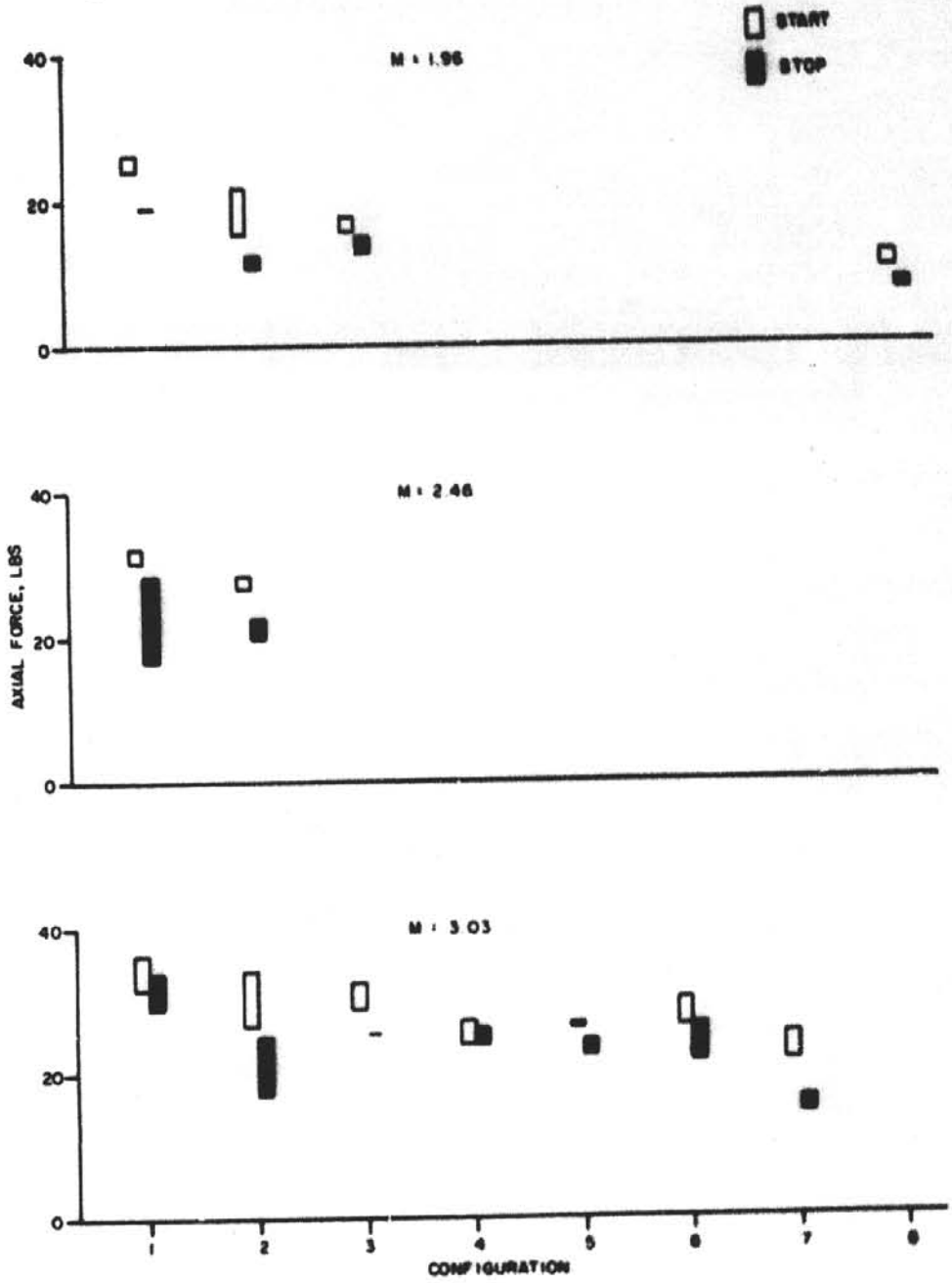

Figure 8. Range of Maximum Measured Axial-Force Starting and Stopping Loads

The ratio of maximum starting loads to steady-state loads (at $\alpha = 0$ degrees) is presented as a function of Mach number in Figure 9. The measured steady-state loads were decreased by the ratio of q_s/q for this load ratio comparison. The data indicate an increase of load ratio with Mach number; a maximum transient axial force of approximately 3-1/2 times the steady-state axial force was observed at Mach 3.

The present data are compared with starting load data taken in the Ordnance Aerophysics Laboratory[5] 19- by 27.5-inch continuous tunnel (Figure 9). The OAL starting loads are considerably higher than the present data, especially above a Mach number of 2.5. A possible explanation for this difference is that the OAL models are low-drag shapes, whereas the Sandia models are basically high-drag shapes (Figure 4). During the transient starting process, the percentage increase (above steady state) of wave or pressure drag should be higher on the low-drag shapes. Hence, the validity of comparing axial-force data for different model shapes on this basis appears questionable.

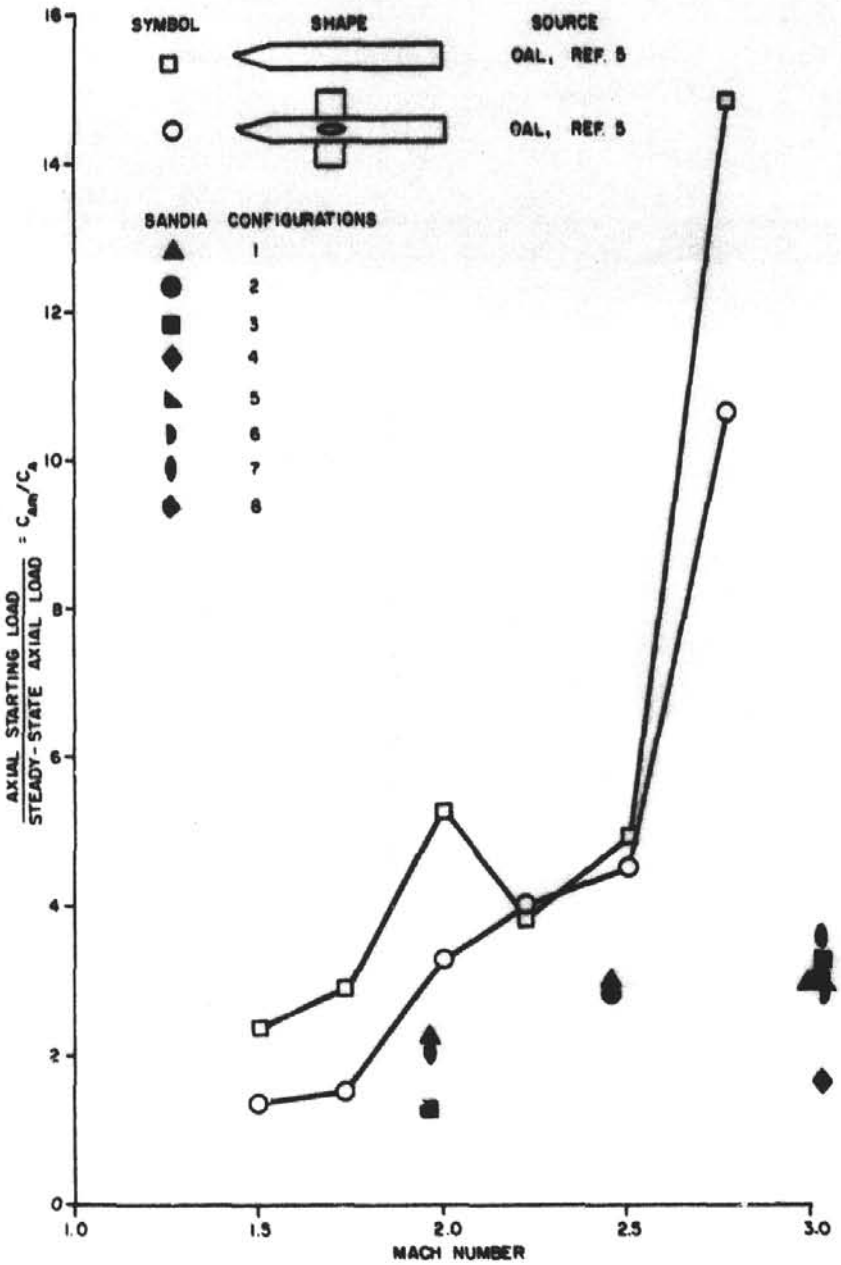

Figure 9. Effect of Mach Number and Model Shape on the Ratio of Starting to Steady-State Axial-Force Loads

Normal Loads

The range of maximum measured normal forces for the eight configurations at the three test Mach numbers is presented in Figure 10. The peak load (whether negative or positive) was determined for each run; each block or bar in Figure 10 represents the variation in these peak loads for the number of runs shown in Table III. Comparison of the positive versus the negative loads (not presented herein) indicated the randomness of the starting load phenomenon and that the tunnel flow is symmetrical; i.e., the range of negative loads was approximately equal to the range of positive loads.

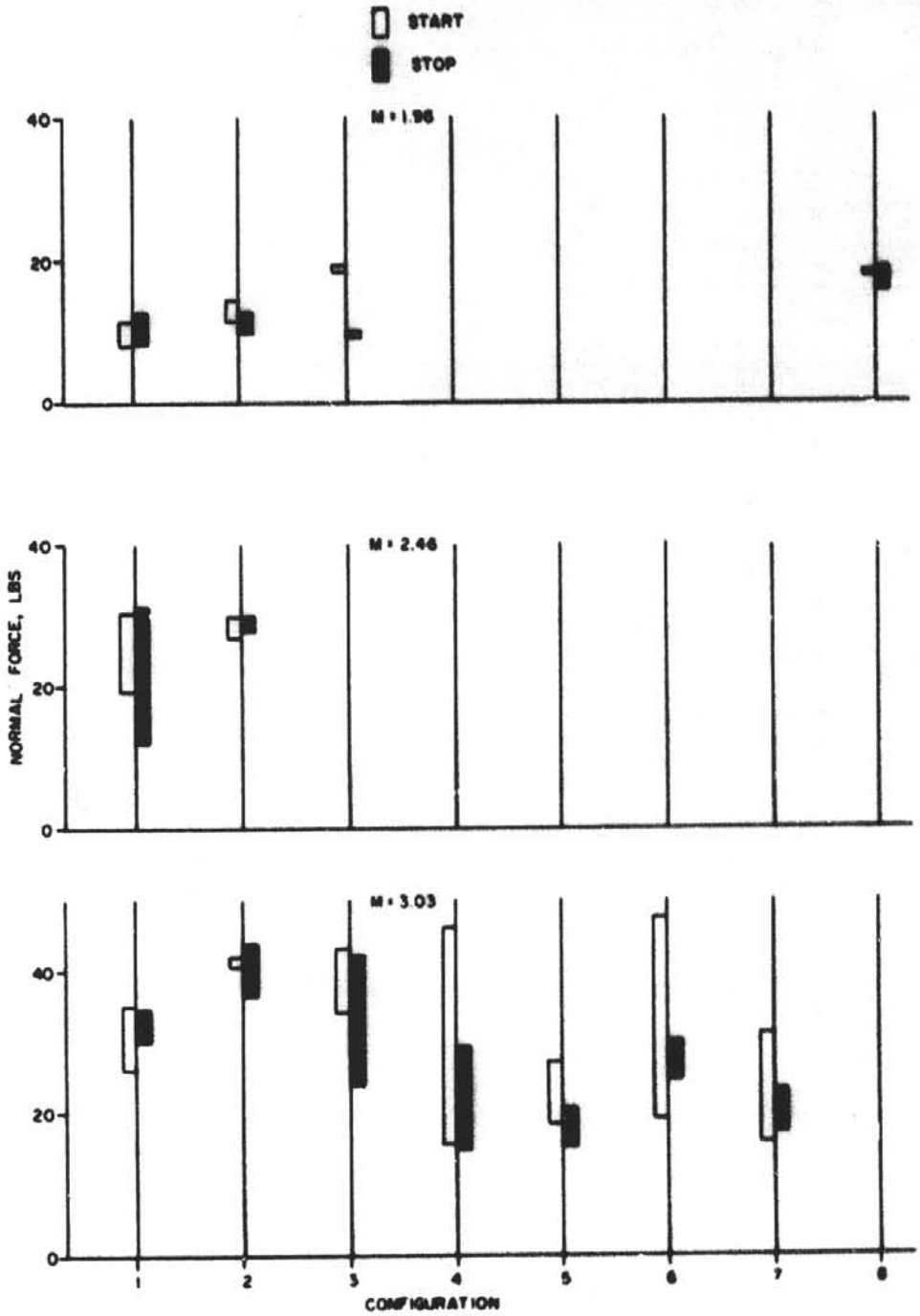

Figure 10. Range of Maximum Measured Normal-Force Starting and Stopping Loads

The ratio of starting loads (at $\alpha = 0$ degrees) to steady running loads* (at $\alpha = 10$ degrees) for four configurations is presented in Figure 11 as a function of Mach number. Data on body alone, wing alone, and wing-body models from the Ordnance Aerophysics Laboratory[5] continuous tunnel are compared with the present data in Figure 11. These normal-force data correlate fairly well.

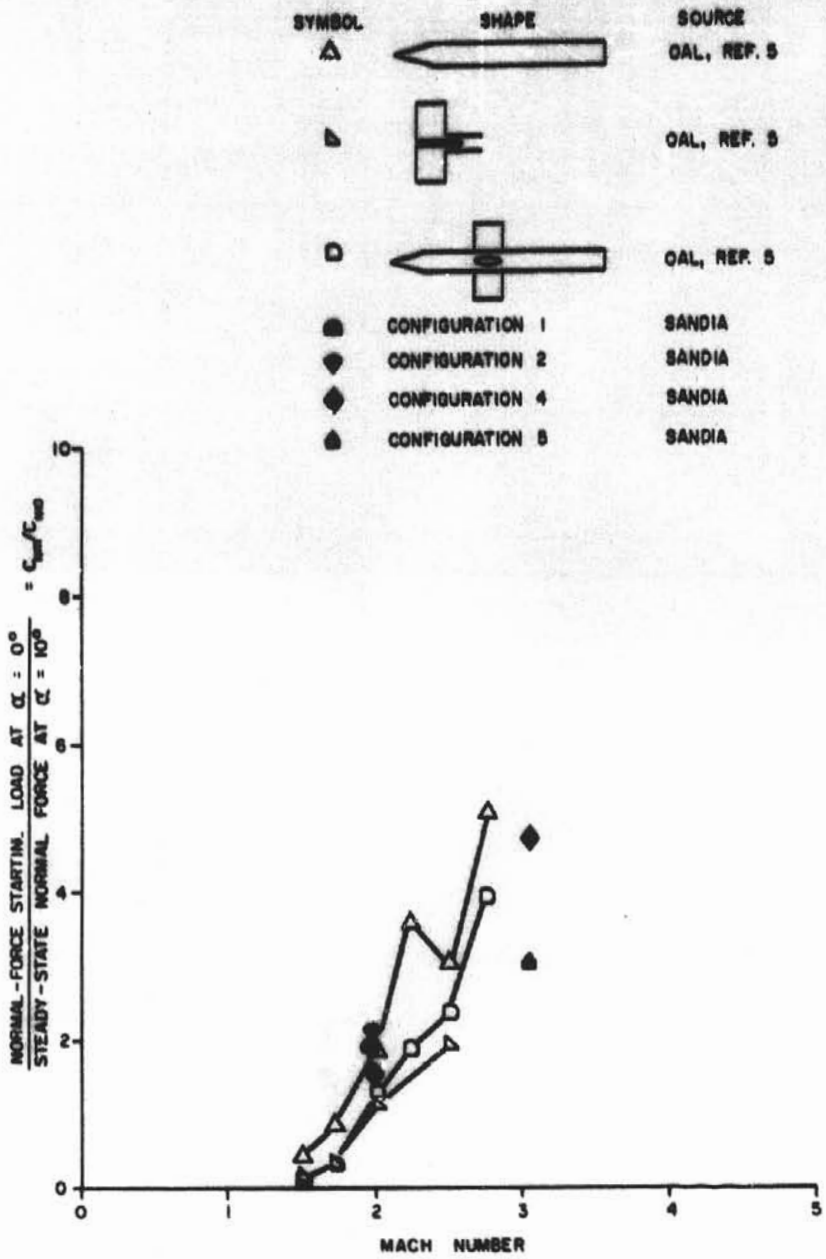

Figure 11. Effect of Mach Number and Model Shape on Ratio of Starting to Steady-State Normal-Force Loads

*The steady-state data for configurations 1, 2, 4, and 5 were obtained during previous three-component force tests in this facility.

The stopping load data for four configurations are compared on the same basis with data from OAL[5] in Figure 12. The stopping loads for the OAL body-alone model are considerably higher (above Mach number 2) than the Sandia and other OAL stopping load data.

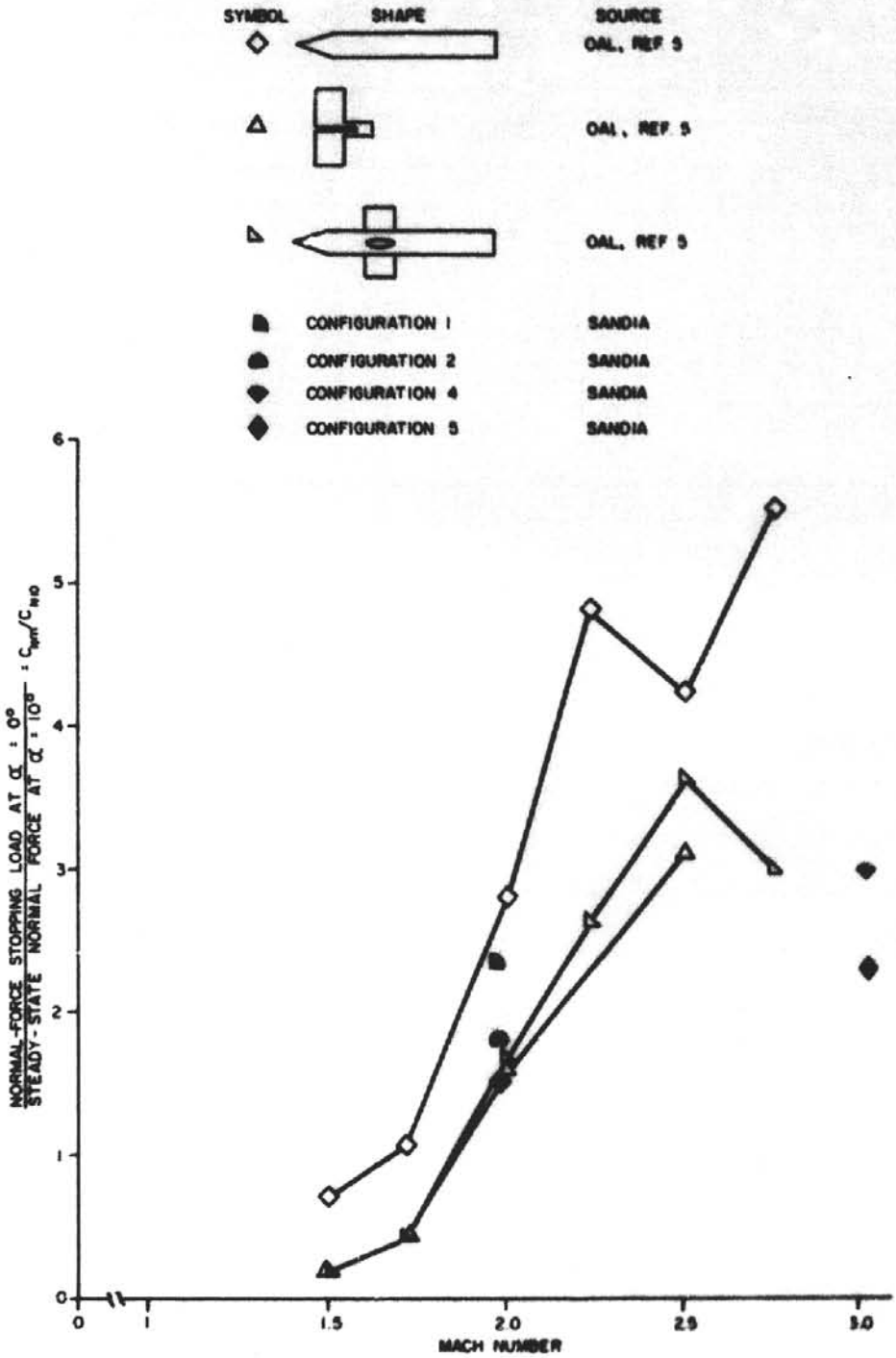

Figure 12. Effect of Mach Number and Model Shape on Ratio of Stopping to Steady-State Normal-Force Loads

Normal-Shock Method Modification

The original "normal-shock" method (Equation 2) is revised by using total model planform area (rather than lifting surface area) to define the normal-force coefficient. This revision (Equation 3) allows correlation of starting load data on the variety of models from bodies of revolution to wing-alone models. However, the mathematical model for the normal-shock method (which essentially assumes an infinite aspect ratio, thin flat plate) is inconsistent with the flow field about a body of revolution during a tunnel start. Cross flow would reduce the pressure difference (assumed normal shock below and attached shock above the model), resulting in lower starting loads. Hence, the magnitude of the starting loads should be a function of S_L/S_T (lifting surface area to total planform area); i.e., the cross flow would be maximum at $S_L/S_T = 0$.

Examination of starting load data from several sources,[1,3,8] along with the present data, indicated that, in general, the experimental data were considerably lower than normal-shock method prediction (Equation 3) at Mach numbers up to approximately 2.5. An empirical modification of Equation 3 was derived in an attempt to develop a method which would predict more reasonable loads at the lower Mach numbers and which would account for the area ratio S_L/S_T. This equation is

$$C_{Nc} = \frac{N_c}{S_T P_{ts}} = \frac{2\gamma(M^2-1)}{(\gamma+1)\left(1+\frac{\gamma-1}{2}M^2\right)^{\frac{\gamma}{\beta(\gamma-1)}}} \tag{4}$$

where

$$\beta = \frac{3}{2}\left(\frac{M-1}{M}\right)\left(0.9 + 0.1\frac{S_L}{S_T}\right), \quad 1.0 \le M \le 3.0 \tag{4a}$$

$$\beta = 0.9 + 0.1\frac{S_L}{S_T}, \quad 3.0 \le M \le 5.0. \tag{4b}$$

The range of normal-force starting load data from this investigation, along with data from AEDC[3] on an AGARD B model, are compared with the analytical methods (Equations 3 and 4) in Figure 13. The present data include the range of maximum loads measured on 8 runs (4 configurations), 14 runs (2 configurations), and 18 runs (7 configurations) at Mach numbers of 2, 2.5, and 3, respectively. The AEDC data represent 60, 198, and 36 runs at Mach numbers 2, 3, and 4.5 respectively, on one configuration. The agreement between these data is fair and the modified normal-shock method (Equation 4) is in closer agreement with the data than the normal-shock method (Equation 3).

The maximum normal-force starting loads (in coefficient form) from these tests, along with data from five other sources, are compared with the analytical methods in Figure 14. With the exception of the one data point from Reference 8, values of C_{Nc} computed from Equation 4 appear to be reasonable approximations of the maximum measured loads. The agreement between the measured values is fair, considering the different model shapes, model sizes, and types of tunnels employed in obtaining these data.

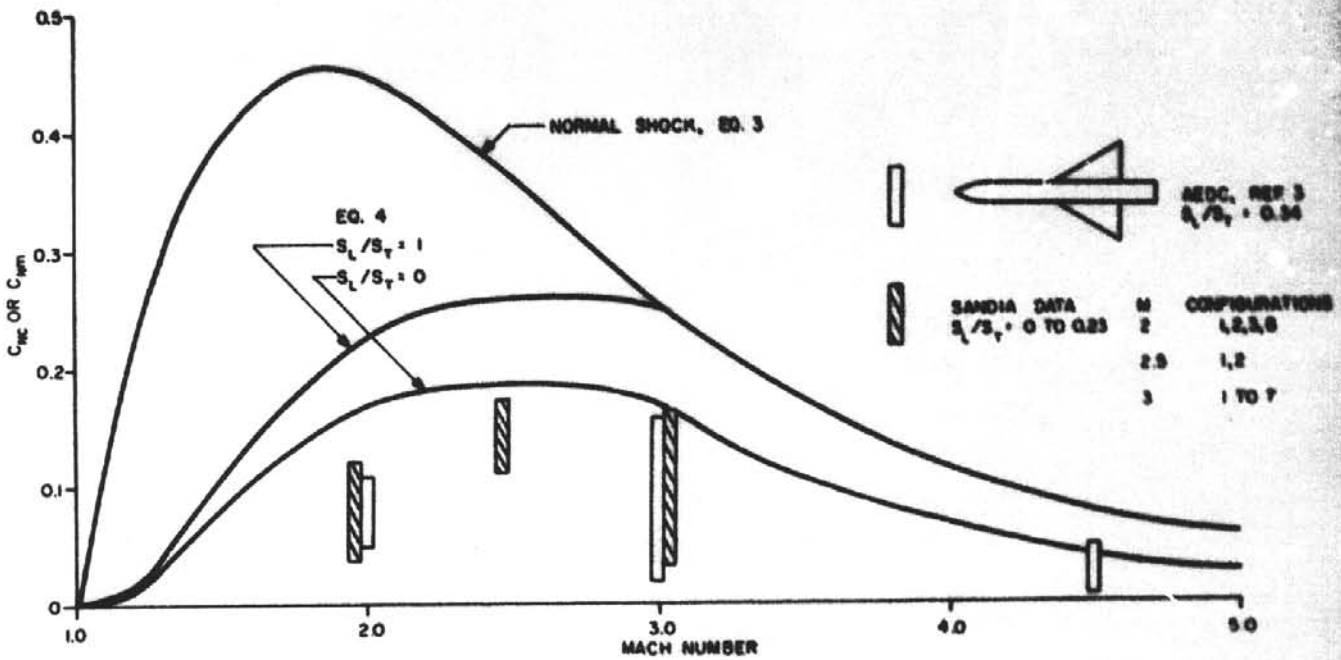

Figure 13. Range of Measured Normal-Force Starting Loads (comparison with AEDC data and empirical method)

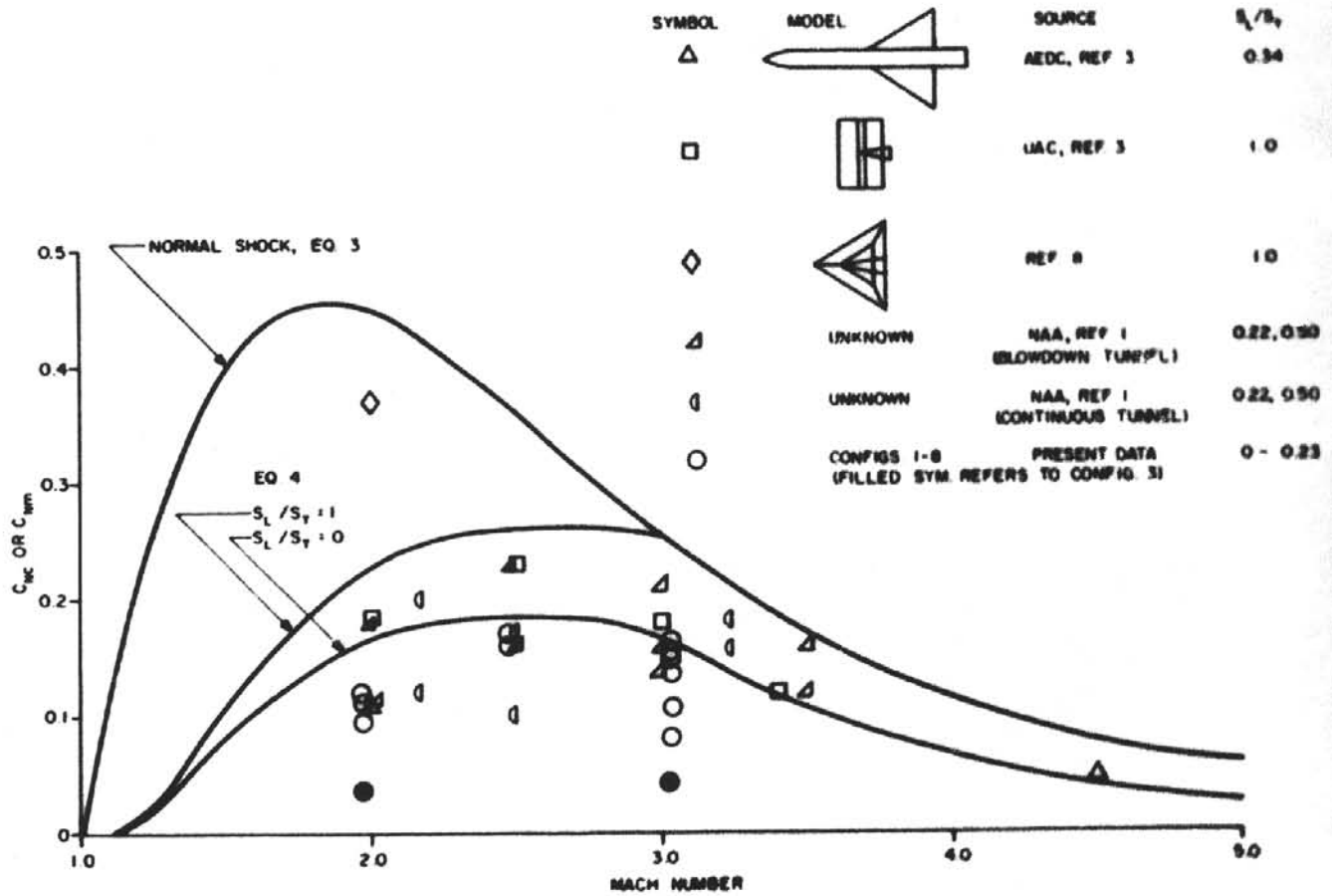

Figure 14. Comparison of Experimental Data with Modified Normal-Shock Methods

The same data are presented in a different manner in Figure 15; the experimental normal force coefficients are plotted versus values calculated from Equation 4. Most of the experimental data fall between the line of perfect correlation* and the line $C_{Nm}/C_{Nc} = 1/2$. A possible reason for the higher experimental data point from Reference 8 is advanced in the next section. The reason for the low starting loads for configuration 3 (solid symbols in Figure 15) is unknown.

On the basis of the data correlations in Figures 14 and 15, Equation 4 will be used to compute the maximum normal-force starting loads for the design of balances, models, etc. in the Sandia facilities.

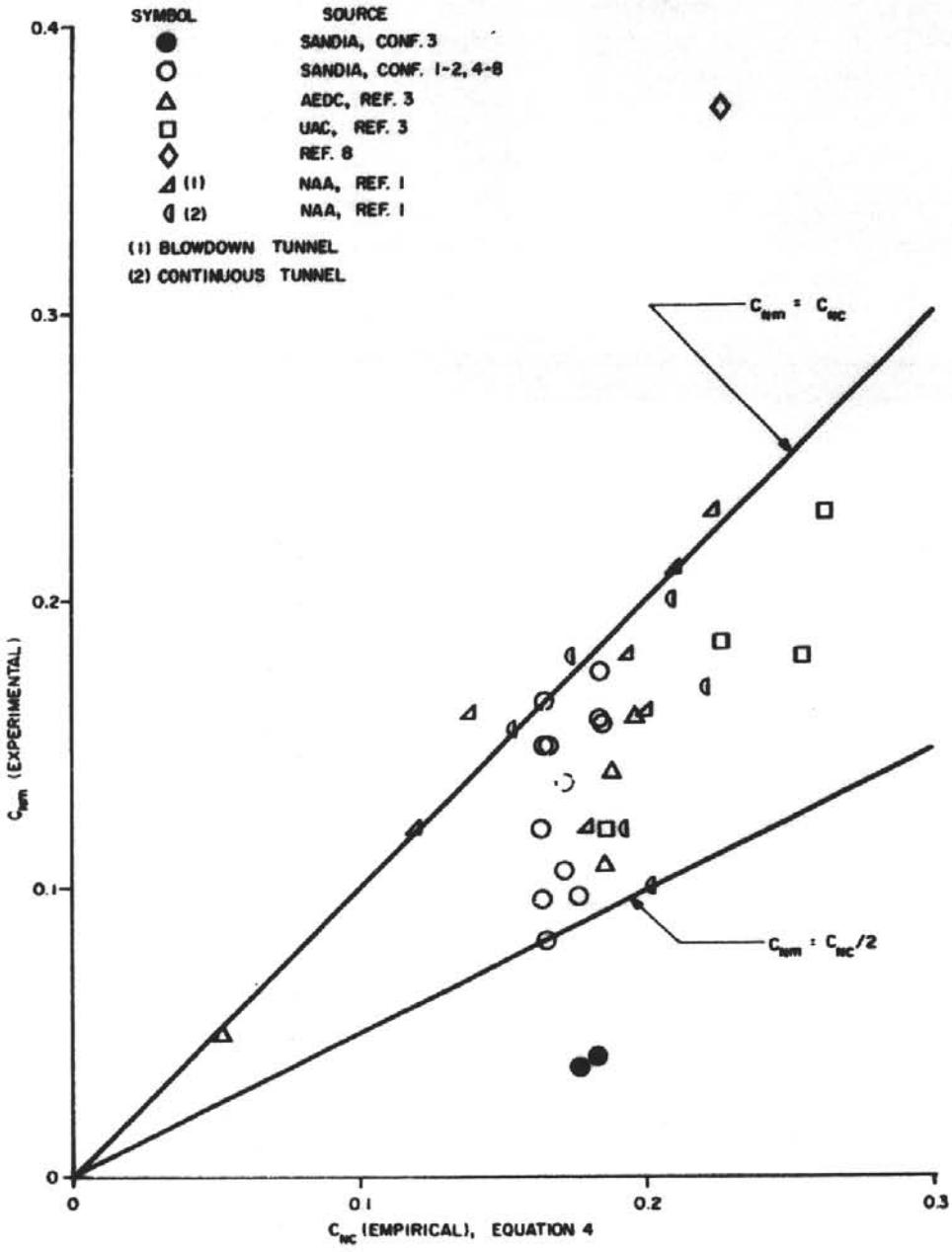

Figure 15. Correlation of Experimental Data with Modified Normal-Shock Method

*The empirical modification (Equation 4) is, in general, conservative.

Frequency and Damping Effects

Wind-off and wind-on measurements of model oscillation frequencies in the axial and normal (vertical) directions indicated that the models oscillated at the natural frequencies during the starting and stopping transients. These natural frequencies are listed in Table II. There are two discernible frequencies in the normal direction; a high frequency due to sting bending is superimposed on the lower frequency oscillation of the balance flexures.

The damping factor (b) was determined from the wind-off oscillograph traces, using the following equation[9]:

$$\ln \theta_m - \ln \theta_{m+1} = \frac{2\pi b}{1-b^2} \tag{5}$$

where m is a given numbered cycle.

These damping factors (for the decay of the lower frequency oscillation, f_{n1}) are listed in Table II.

An attempt was made to measure the forcing frequencies (pressure fluctuations) during the transient starting and stopping in order to ascertain whether conditions were such that the normal-force loads might be magnified by the forcing frequencies. The test section static pressures were measured with a 25-psid Statham pressure transducer mounted on the perforated-wall test section at stations 10 and 24 (see Figure 1). The transducer output was monitored on a Visicorder in a manner similar to that described for balance strain gage output (see Instrumentation). Low-amplitude pressure oscillations in the approximate range of 300 to 1900 cycles per second were recorded at all three Mach numbers during start, stop, and steady-running conditions; these higher frequencies were not considered significant because of the low amplitudes. The approximate values of forcing frequencies* are presented in Table IV.

TABLE IV

Forcing Frequency Data

M	f_f, cycles/sec, during start	f_f, cycles/sec, during stop
2	3.2	3.2
2.5	3.2, 6, 96	3.2, 6, 40, 110
3	3.2, 11, 90, 120	3.2, 6, 10, 65, 100

The frequency of the tunnel organ piping was 3.2 cycles per second. Organ piping is the fore and aft movement of waves (which originate as pressure pulses from control valve movement) between the exhaust stack and the terminal shock system (or the settling chamber if the flow is subsonic).

---

*North American[1] reported forcing frequencies (from tunnel pressure measurements) in the range of 5 to 150 cycles per second.

A plot of relative magnification factor (RM) versus frequency ratio (forcing frequency/natural frequency) with various damping factors (b) for a periodic, forced-vibration (with viscous damping) system[9] is presented in Figure 16. The frequency ratios measured in these tests (from Tables II & IV) at each Mach number during start and stop are plotted in Figure 16, along with a tabulation of the damping factors.

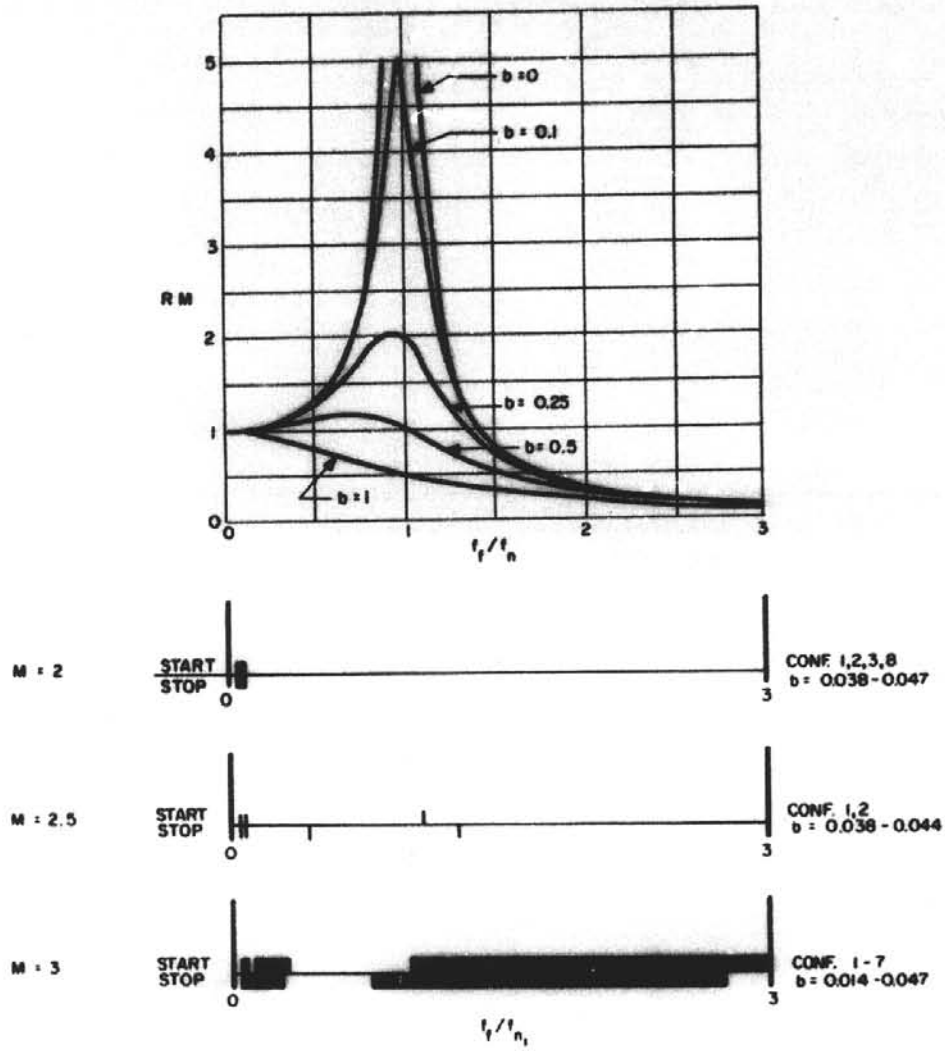

Figure 16. Comparison of the Measured Frequency Ratios and Damping Factors with Ratios for a Forced-Vibration (with viscous damping) System

This qualitative* representation indicates that starting or stopping normal-force load amplification could have occurred at Mach numbers of 2.5 and 3.0, since the frequency ratios are in the resonance range and the damping factors are very small. However, the Mach number 2 data indicate no fore and aft oscillation of the starting shocks which occurred at the other Mach numbers. The symmetrical start (continuous movement of a shock system down the tunnel) probably accounts for the lower normal-force loads measured by several investigators (see Figure 14) than would be predicted by using normal-shock theory (Equation 3). Kinsolving and Jackson[3] indicated that schlieren movies showed symmetrical starts in Tunnel E-1 at M = 2.

The larger normal-force starting load at M = 2 (shown in Figures 14 and 15) from Reference 8 might have been due to an unsymmetrical start and/or frequency ratios near resonance.

Conclusions

Analysis of the transient axial- and normal-force data presented herein and comparison of these data with analytical methods and other data indicate that:

1. In general, the axial- and normal-force starting loads were slightly higher than the stopping loads in the Sandia 1-foot tunnel.

2. The maximum axial-force starting load at $\alpha = 0$ degrees was approximately 3-1/2 times the steady-state running load at $\alpha = 0$ degrees for M = 3 in this facility; the maximum normal-force starting load at $\alpha = 0$ degrees was approximately 5 times the steady-state running load at $\alpha = 10$ degrees for M = 3.

3. The models oscillated at the natural frequencies of the model-balance-sting system during the occurrence of the peak transient loads in this facility; measurements of test section pressure transients indicated symmetrical starts at M = 2 and nonsymmetrical (fore and aft oscillation of the shock system) at M = 2.5 and M = 3.

4. These maximum normal-force starting load data correlate fairly well with data from other tunnels for a variety of model shapes when the coefficients are calculated on an equivalent basis; i.e., use of total model planform area as the reference area.

5. The magnitude of the normal-force starting load appears to be a function of S_L/S_T (lifting surface area/planform area).

6. An empirical modification of the "normal-shock" method allows a degree of correlation of the maximum starting loads measured on a variety of model shapes at six supersonic wind tunnels.

---

*These two forced vibration systems are somewhat dissimilar, since the forcing function pressure oscillations (Table IV) last only a few cycles and are not truly periodic compared with the harmonic shaking force acting on the vibrating mass for the ideal system.

LIST OF REFERENCES

1. Gorowitz, H., "North American Aviation, Incorporated 7x7 Foot Trisonic Wind Tunnel: Summary of Wind Tunnel Starting Load Studies," 11th Meeting of Supersonic Tunnel Association, April 1959.

2. Schreiber, R. E., Transient Behavior of the Boeing Supersonic Wind Tunnel and Means for Reducing Attendant Starting and Stopping Loads, paper presented at the AGARD-STA Meeting, Marseilles, France, September 1959.

3. Kinsolving, S. L., and Jackson, R., Starting Loads in an Intermittent Supersonic Wind Tunnel, AEDC-TN-59-6, January 1959.

4. Winter, K. G., and Brown, C. S., Loads on a Model During Starting and Stopping of an Intermittent Supersonic Wind Tunnel, RAE TN AERO. 2453, May 1956.

5. Goin, K. L., Summary Calibration Report of the Ordnance Aerophysics Laboratory Supersonic Wind Tunnel, OAL Report 340-2, August 1957.

6. Davis, M. W., and Peterson, K. A., Airflow Calibration of the Sandia Corporation 12-Inch Transonic Tunnel, SC-4104(TR), June 1957.

7. Tolbert, C. C., Mechanical Operations Manual for the Sandia Corporation Twelve-Inch Wind-Tunnel Facility, SC Technical Memorandum 290-56-51, January 1957.

8. Erdman, S. F., Starting Loads in Supersonic Wind Tunnels - Some Experiences, paper presented at Aeronautical Seminar KTH Stockholm, 1954.

9. Myklestad, N. O., Vibration Analysis, McGraw Hill Book Company, 1944.

DISTRIBUTION:

Librarian, DMA, Washington 25, D.C.
K. F. Hertford, AEC-ALO
W. L. Hancock, AEC-SAO
N. E. Bradbury, LASL
DTIE, Oak Ridge, Tennessee (325)
OTS, Washington 25, D. C. (75)
H. F. Carroll, Chief, Classification Division, AEC-Oak Ridge
R. S. Claassen, 5100
G. A. Fowler, 7000
H. E. Lenander, 7100
V. E. Blake, 7110
J. W. Jones, 7120
A. Y. Pope, 7130
R. S. Wilson, 7140
H. H. Patterson, 7160
S. A. Moore, 7180
H. R. Vaughn, 7131
R. C. Maydew, 7132
K. F. Crowder, 7133
W. H. Curry, 7134
W. T. Botner, 7132-1
J. F. Reed, 7132-2
K. L. Goin, 7132-3
E. C. Rightley, 7133-2
W. J. Howard, 8100
Mrs. B. R. Allen, 3421-1
Mrs. M. G. Randle, 3421-2
R. K. Smeltzer, 3421-3
W. A. Jamieson, 8233
W. F. Carstens, 3423
R. C. Smelich, 3446-1 (5)
TISE, Aero-Thermodynamics Standard Distribution (174)